Precise Tuning of Porosity and Surface Functionality in Au@SiO_2 Nanoreactors for High Catalytic Efficiency

Joongoo Lee, Ji Chan Park, Jung Up Bang, and Hyunjoon Song*

Department of Chemistry and School of Molecular Science (BK21), Korea Advanced Institute of Science and Technology, Daejeon 305-701, Korea

Received April 28, 2008. Revised Manuscript Received July 8, 2008

Nanoreactor frameworks have many advantages over bulk catalyst structures in terms of providing a regular reaction environment and conformational stability. In this work, Au@SiO_2 nanoreactor frameworks were chemically modified to improve the catalytic efficiency of *o*-nitroaniline reduction. The porosity of silica shells was readily controlled by introducing C_{18}TMS as a porogen with heat treatment. The diffusion rate of the silica layers was tuned from 5.9×10^{-19} to 2.1×10^{-18} m^2 s^{-1}, which directly altered the turnover frequency and rate constant of the reaction. Carboxylate functionality was introduced on the gold cores of Au@SiO_2 nanoreactors by 3-MPA addition. The reaction rate was enhanced by a maximum of 2.4 times compared to unfunctionalized catalysts through a strong interaction between carboxylate anions and o-nitroaniline. Totally, the rate constant of Au@SiO_2 yolk−shell nanoreactors exhibits a 13-fold enhancement by diffusion and surface functionality control. These results indicate that the rational design of a nanoreactor framework with appropriate chemical functionalization can maximize the catalytic efficiency of various solution-phase reactions.

Introduction

Improving the efficiency of metal-based catalysts is a high priority issue in various industries because of the high cost and limited supply of metal components. For high catalytic efficiency, it is necessary to reduce metal particle sizes and thereby increase surface areas and active sites such as edges and kinks.[1] The general form of heterogeneous catalysts is tiny metal particles embedded on silica and metal oxide supports, because highly active metal nanoparticles are effectively stabilized by high surface area supports.[2] The supports prevent particle aggregation and, in some cases, form new active components on the interface with metals.[3]

Recently, Somorjai et al. introduced a Pt@CoO nanoreactor framework, a new type of bifunctional catalyst system.[4] The framework incorporates platinum particles inside polycrystalline CoO hollow shells, and runs ethylene hydrogenation reactions. We have also demonstrated Au@SiO_2 yolk−shell nanoreactors as a model catalyst for the catalytic reduction of *p*-nitrophenol.[5] These metal@metal oxide nanoreactor frameworks are structurally analogous to metal particles embedded on mesoporous silica, such as metal/MCFs (mesocellular foams).[6] However, a major difference from the metal/silica structure is complete isolation of the active metal nanoparticles by solid shells, which offers many advantages for catalytic reactions. Each nanoparticle has a homogeneous environment surrounded by a single metal oxide shell. The diffusion rate of the silica shells in Au@SiO_2 nanoreactors is almost identical throughout all catalyst particles, whereas those of the metal/silica structure have broad distributions, from deeply buried metal nanoparticles to particles embedding on the outward surface of mesoporous silica. The solid shells of Au@SiO_2 can serve as a shield for limiting conformational variations of the particles. The particle aggregation often occurs during the reaction and discriminates reaction properties in bulk catalysts.[7]

In addition, the nanoreactor framework is a well-defined system, and thus precise structural and functional control by appropriate chemical modification is plausible for both metal particles and metal oxide shells. Porosity of the supports directly influences their surface area and catalyst dispersion, as well as the reagents' diffusion rates, resulting in distinct catalytic properties. The porosity control of silica mesostructures has been widely studied using various surfactants, soft templates, additives, and reaction conditions.[8] Generally, porogens are introduced into the reaction mixture to form heterogeneous domains and generate a number of pores inside the silica structure by thermal or chemical treatment.[9] Long alkyl siloxanes such as C_{18}TMS (octadecyltrimethoxysilane) have been used as effective porogens to synthesize porous silica coatings, where the relative concentration ratio of the porogen to the silica precursor can be varied so as to adjust pore densities and diffusion rates of the silica layers.[9,10]

Careful design of the surface functionality appears to be a requirement for high catalytic efficiency of the

* Corresponding author. E-mail: hsong@kaist.ac.kr.

(1) Zhou B.; Hermans, S.; Somorjai, G. A. *Nanotechnology in Catalysis*; Kluwer Academic: New York, 2004.
(2) Bell, A. T. *Science* **2003**, *299*, 1688.
(3) Zhu, J.; Sormorjai, G. A. *Nano Lett.* **2001**, *1*, 8.
(4) Yin, Y.; Rioux, R. M.; Erdonmez, C. K.; Hughes, S.; Somorjai, G. A.; Alivisatos, A. P. *Science* **2004**, *304*, 711.
(5) Lee, J.; Park, J. C.; Song, H. *Adv. Mater.* **2008**, *20*, 1523.
(6) Kuœtrowsk, P.; Chmielarz, L.; Dziembaj, R.; Cool, P.; Vansant, E. F. *J. Phys. Chem. B* **2005**, *109*, 11552.
(7) Narayanan, R.; El-Sayed, M. A. *J. Am. Chem. Soc.* **2003**, *125*, 8340.
(8) Wan, Y.; Zhao, D. *Chem. Rev.* **2007**, *107*, 2821.
(9) Kim, J. Y.; Yoon, S. B.; Yu, J.-S. *Chem. Commun.* **2003**, 790.
(10) Yano, K.; Fukushima, Y. *J. Mater. Chem.* **2004**, *14*, 1579.

10.1021/cm801149w CCC: $40.75
Published on Web 08/23/2008

Scheme 1. Synthesis and Chemical Functionalization of $Au@SiO_2$ Nanoreactor Frameworks

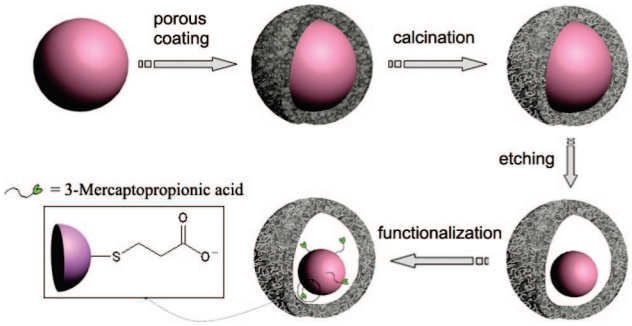

reaction. It is noted that most biologically important enzymes use similar strategies; the reaction runs at the active metal center, and the residues close to the center help to stabilize reaction intermediates by hydrogen bonding and electrostatic interactions and thereby significantly accelerate the reaction rates.[11] For metal particles, self-assembled monolayers (SAMs) can provide various functionalities on the metal surface.[12] Specific functional groups can act as molecular recognition sites of incoming reagents.[13] They can either enhance the reaction rates by increasing the retention time of the reactants or block the active surface from unwanted reagents.

In the present work, we have controlled the porosity of silica shells in $Au@SiO_2$ nanoreactor frameworks by introducing $C_{18}TMS$ as a porogen. Different amounts of $C_{18}TMS$ with respect to the silica precursor concentration altered the porosity and diffusion rates of the silica shells, and influenced the overall reaction rates of *o*-nitroaniline (*o*-NA) reduction. We have also demonstrated the effect of surface functionality on the reaction rates. Gold cores of the $Au@SiO_2$ catalysts anchored 3-mercaptopropionic acid (3-MPA), which enhanced the reaction rates by a maximum of 2.4 times through hydrogen bonding with the reactants. Scheme 1 summarizes the chemical control of porosity and surface functionality in the $Au@SiO_2$ nanoreactor frameworks.

Experimental Section

Reagents. Hydrogen tetrachloroaurate(III) trihydrate ($HAuCl_4 \cdot 3H_2O$, 99.9+%), silver nitrate ($AgNO_3$, 99+%), poly(vinyl pyrolidone) (PVP, $M_w = 55\,000$), 1,5-pentanediol (PD, 96%), tetraethylorthosilicate (TEOS, 98%), octadecyltrimethoxysilane ($C_{18}TMS$, 90%), 3-mercaptopropionic acid (3-MPA, 99+%), potassium cyanide (KCN, 97%), and sodium borohydride ($NaBH_4$, 99%) were purchased from Aldrich. 2-Propanol (99.5%) and ammonium hydroxide (NH_4OH, 28% in water) were obtained from Junsei. Ethanol (99.9%) and *o*-nitroaniline (*o*-NA, 98%) were purchased from J. T. Baker and Acros, respectively. The reagents were used as received without further purification.

$Au@SiO_2$ Core−Shell Nanoparticles. Gold nanoparticles were prepared by a modified polyol process according to the literature.[14]

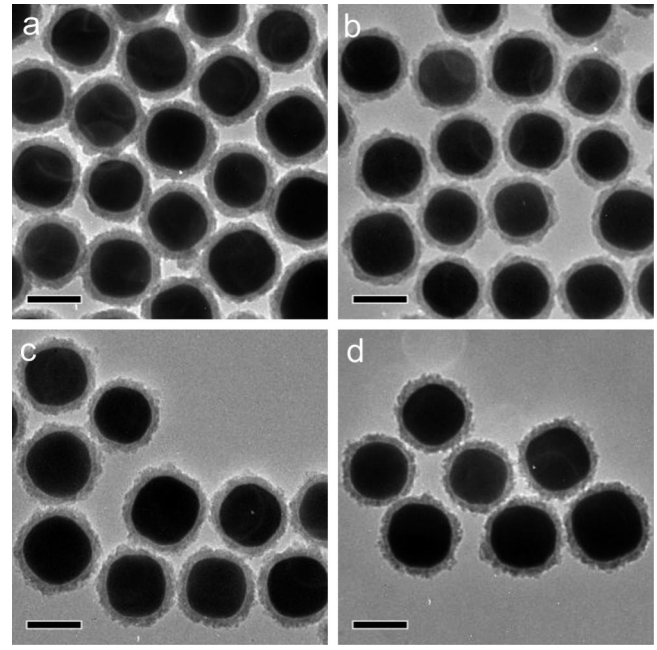

Figure 1. TEM images of diffusion-controlled $Au@SiO_2$ core−shell particles. The concentration ratios of $C_{18}TMS$ and TEOS used for the synthesis, [$C_{18}TMS$]/[TEOS], were (a) 0.06, (b) 0.08, (c) 0.10, and (d) 0.12, respectively. The bars represent 100 nm.

A mixture of ammonium hydroxide aqueous solution (0.4 mL) and 2-propanol (9.4 mL) was added to the gold nanoparticle dispersion (10 mL, 9.6×10^{-4} M with respect to the original gold precursor concentration; 1.4×10^{11} particles) in ethanol. After 30 s, a mixture of deionized water (3.0 mL), TEOS (25 μL), and $C_{18}TMS$ in 2-propanol (1.8 mL) was added, and the reaction mixture was vigorously stirred for 1.5 h to ensure complete polymerization of silica on the gold surface. The amounts of $C_{18}TMS$ used in the reactions were 3.0, 4.0, 5.0, and 6.0 μL, in order to set the [$C_{18}TMS$]/[TEOS] equivalent to 0.06, 0.08, 0.10, and 0.12, respectively. The core−shell particles were precipitated by centrifugation at 6000 rpm for 10 min, and washed thoroughly with ethanol. The particles were dried in a vacuum oven for 1 h at 373 K and calcined in a tube furnace at 773 K for 2.5 h in air. Finally, the $Au@SiO_2$ particles were dispersed in 2-propanol by brief sonication to set the concentration as 3.6×10^{-3} M with respect to the gold precursor concentration.

$Au@SiO_2$ Yolk−Shell Nanoreactors. The $Au@SiO_2$ core−shell particle dispersion (0.5 mL, 3.6×10^{-3} M with respect to the gold precursor concentration; 1.1×10^{10} particles) was added to water (5.0 mL). A KCN aqueous solution (0.3 mL, 0.01 M) was added and the reaction mixture was stirred for 10 min at room temperature. The particles were precipitated by centrifugation at 6000 rpm for 10 min and washed with 2-propanol thoroughly.

Estimation of the Diffusion Coefficient of Silica Layers. The $Au@SiO_2$ yolk−shell particle dispersion in 2-propanol (0.50 mL, 7.4×10^{-4} M with respect to the gold precursor concentration; 5.5×10^9 particles) was immediately added into a mixture of 2-propanol (2.0 mL) and quinoline (30 μL) inside a cuvette mounted on a UV−vis spectrometer. The extinction change was monitored at intervals of 30 s to ~1 min. The diffusion kinetics were analyzed according to a method reported in the literature using the peak position change versus time (Figure 3c).[15] The effective refractive index (n_{eff}) of the surrounding medium can be defined as

(11) Li, T.; Lee, H.; Park, K. *J. Biomater. Sci., Polym. Ed.* **1998**, *9*, 327.
(12) Love, J. C.; Estroff, L. A.; Kriebel, J. K.; Nuzzo, R. G.; Whitesides, G. M. *Chem. Rev.* **2005**, *105*, 1103.
(13) Tengvall, P.; Lestelius, M.; Liedberg, B.; Lundström, I. *Langmuir* **1992**, *8*, 1236.
(14) Giersig, M.; Ung, T.; Liz-Marzán, L. M.; Mulvaney, P. *Adv. Mater.* **1997**, *9*, 570.
(15) Kamata, K.; Lu, Y.; Xia, Y. *J. Am. Chem. Soc.* **2003**, *125*, 2384.

$$n_{\text{eff}} = (1 - V_f)n_{\text{2-propanol}} + V_f n_{\text{quinoline}} \quad (1)$$

where $n_{\text{2-propanol}}$ (1.377) and $n_{\text{quinoline}}$ (1.62) are the refractive indexes of 2-propanol and quinoline, respectively, and V_f is the volume fraction of 2-propanol escaping from the silica shell.

The relation between V_f ($= n_t/n_\infty$) and the square root of time is as follows

$$n_t/n_\infty = 6(Dt/\pi R^2)^{1/2} \quad (2)$$

where D is the diffusion coefficient and R is the radius of the silica hollow shell (59.5 nm). The diffusion coefficient of the silica layers can be calculated from the rewritten form

$$D = (\pi R^2/36)(V_f^2/t) \quad (3)$$

where (V_f^2/t) is the square of the line slope from the linear relation between n_t/n_∞ and the square root of time. The diffusion coefficient of silica layers in the Au@SiO$_2$ yolk−shell nanoreactors is estimated from this equation for Au@SiO$_2$ yolk−shell nanoreactors with different porosity.

Catalytic Reduction of *o*-NA. The solvent (2-propanol) of the Au@SiO$_2$ nanoreactor dispersion was replaced with water. The Au@SiO$_2$ nanoreactor dispersion in water (1.0 mL, 7.4×10^{-4} M with respect to the gold precursor concentration; 1.1×10^{10} particles) was added to a $NaBH_4$ aqueous solution (1.0 mL, 1.2 M), and the mixture was stirred for 30 min at room temperature. *o*-NA aqueous solution (1.0 mL, 3.4×10^{-3} M) was added, and the resulting mixture was stirred at room temperature until the yellow solution became colorless. The reaction progress was monitored by taking a small portion of the reaction mixture every 3 min for each reaction.

Calculation of the Rate Constants. The amount of molecules transferred into the silica shell was calculated under the assumptions that the concentrations of *o*-NA inside and outside silica were constant and a concentration gradient was generated only in the silica shell.

$$V_{\text{outside}}(C_{\text{out},0} - C_{\text{out,t}})/t = A_{\text{outside}}(D_{\text{eff}}/l)(C_{\text{out}} - C_{\text{in}}) \quad (4)$$

$$A_{\text{outside}}(D_{\text{eff}}/l)(C_{\text{out}} - C_{\text{in}}) = k_{\text{Au}} C_{\text{in}} V_{\text{inside}} \quad (5)$$

where l is the shell thickness (17 nm), V_{outside} and A_{outside} are the volume and surface area of the Au@SiO$_2$ particles (68 nm radius), and V_{inside} is the volume of empty space inside the silica. $C_{\text{out},0}$, $C_{\text{out,t}}$, and C_{in} are the concentration outside the silica shell at the initial time, after t seconds, and the concentration inside the silica shell, respectively. D_{eff} is the diffusion coefficient calculated from eq 3. C_{in} was calculated via eq 4, and k_{Au}, the rate constant on the gold surface, was obtained from eq 5.

Functionalization of the Gold Cores with 3-MPA. Appropriate amounts of 3-MPA (0.50, 1.0, 2.0, 4.0, 6.0, and 8.0 mmol) in ethanol (1.0 mL) were added to the Au@SiO$_2$ yolk-shell particle dispersion in 2-propanol (1 mL, 7.4×10^{-4} M with respect to the gold precursor concentration; 1.1×10^{10} particles), in which the particles were prepared under a condition of [C_{18}TMS]/[TEOS] = 0.12. The reaction mixture was stirred for 24 h. The particles were separated by centrifugation at 6000 rpm for 10 min and washed thoroughly with ethanol.

Characterization. Transmission electron microscopy (TEM) images were obtained on a Philips CM-20 operated at 240 kV using samples prepared by placing a few drops of the dispersion on copper grids coated with a lacey carbon film (Ted Pella, Inc.) The UV−vis measurements were carried out on a Jasco V530 UV−vis spectrophotometer using colloidal dispersions in 2-propanol.

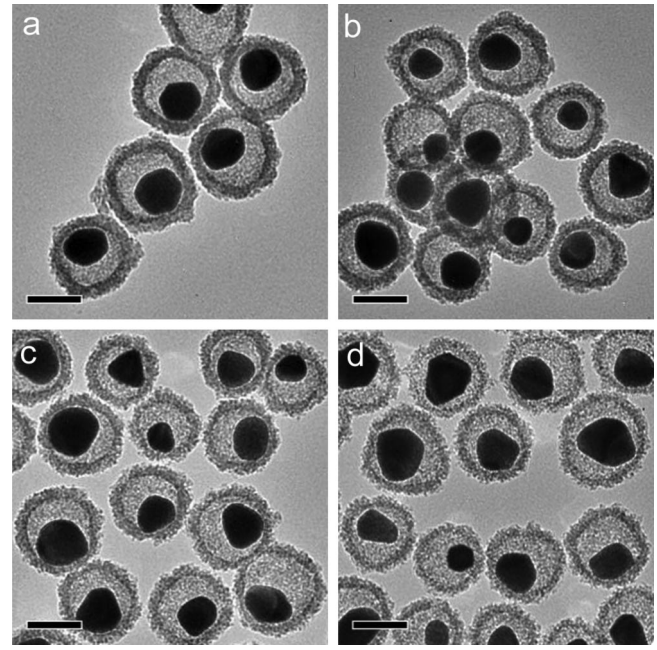

Figure 2. TEM images of diffusion-controlled Au@SiO$_2$ yolk−shell nanoreactors. The [C_{18}TMS]/[TEOS] ratios used for the synthesis were (a) 0.06, (b) 0.08, (c) 0.10, and (d) 0.12, respectively. The bars represent 100 nm.

Results and Discussion

Porosity Control of Au@SiO$_2$ Nanoreactor Frameworks. The basic structure of Au@SiO$_2$ nanoreactor frameworks was reported in previous works.[5,14] Gold nanoparticles were prepared by a modified polyol process in the presence of poly(vinyl pyrrolidone) (PVP) as a surfactant.[16] The gold particles were coated with silica shells through the Stöber method.[17] For the porosity control of silica shells, an appropriate amount of C_{18}TMS as well as TEOS (tetraethylorthosilicate) was added to the gold colloidal dispersion in ethanol. The addition of siloxane with a long alkyl chain led to sparse silica polymerization, and generated pores inside the silica networks.[9] The molar ratios of C_{18}TMS used in the reaction with respect to the silica precursor concentration were 0.06, 0.08, 0.10, and 0.12. After the silica shells were coated completely, the Au@SiO$_2$ core−shell particles were calcined at 773 K for 2.5 h in air to remove organic moieties. Transmission electron microscopy (TEM) images of the Au@SiO$_2$ particles after heat treatment (Figure 1) show that the silica shells are uniformly coated on the spherical gold particles. The sizes of the cores and shells are almost identical for all samples, where the average diameters of the gold cores are estimated to be 102 ± 8 nm with silica shell thicknesses of 17 ± 2 nm. The surface of the silica shells becomes rougher as the molar ratio of C_{18}TMS is increased, because of the sparse and irregular polymerization of the silica networks.

Au@SiO$_2$ yolk−shell nanoreactors with smaller cores were fabricated by selective etching of the gold cores of the Au@SiO$_2$ core−shell particles. The addition of KCN stoichiometrically oxidized Au(0) to $Au(CN)_2^-$ ions, which were

(16) Seo, D.; Park, J. C.; Song, H. *J. Am. Chem. Soc.* **2006**, *128*, 14863.
(17) Stöber, W.; Fink, A.; Bohn, E. *J. Colloid Interface Sci.* **1968**, *26*, 62.

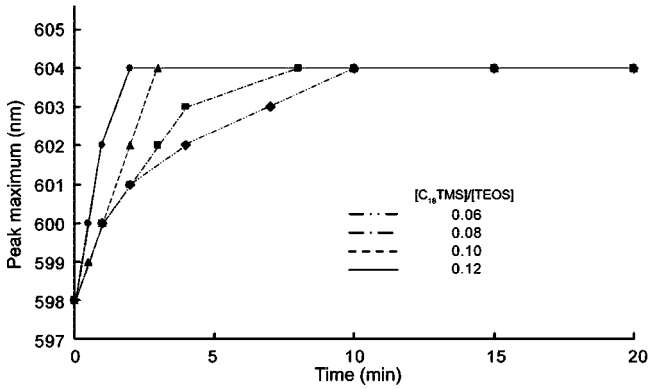

Figure 3. UV−vis extinction changes of Au@SiO_2 yolk−shell colloidal dispersion in 2-propanol added to a mixture of 2-propanol and quinoline.

Table 1. Diffusion Coefficients and Turnover Frequencies (TOFs) of the Au@SiO_2 Yolk−Shell Nanoreactor Frameworks[a]

[C_{18}TMS]/[TEOS]	diffusion coefficient ($m^2\ s^{-1}$)	TOF (s^{-1})[b]
0.06	5.9×10^{-19}	5.1
0.08	8.5×10^{-19}	11
0.10	1.1×10^{-18}	14
0.12	2.1×10^{-18}	35

[a] The same number of particles (1.1×10^{10}) was used for each reaction. [b] TOF was calculated from the corresponding spheres with the mean atomic diameter (135 pm) of bulk gold metals.

dissolved in solution.[14] Figure 2 shows that gold cores with average diameters of 76−80 nm were generated by the addition of KCN aqueous solution (0.01 M, 0.3 mL) without changing the spherical shell structures. The size distributions of the etched gold cores are relatively large (~16%) compared to those of gold nanoparticles synthesized by a polyol process, due to the fast diffusion of cyanide ions and irregular dissolution of the gold cores through porous silica shells. The rough surface of the silica hollows is clearly represented in the TEM images.

The diffusion rates, which are related to the concentration ratios of C_{18}TMS and TEOS used for the catalyst synthesis ([C_{18}TMS]/[TEOS]), were evaluated by UV−vis spectroscopy. The surface plasmon resonance of metal particles is known to be sensitive to the refractive index of the surrounding media. The UV−vis extinction peak of Au@SiO_2 yolk−shell particles in 2-propanol (refractive index (n) = 1.377) appears at 598 nm. The Au@SiO_2 particle dispersion in 2-propanol was immediately added to a mixture of quinoline (n = 1.62) and 2-propanol, and the extinction changes were monitored at a regular time interval of 30 s to 1 min (Figure 3). The UV−vis peak maximum was gradually shifted to 604 nm by the exchange of 2-propanol to quinoline inside the silica shells. This 6 nm red-shift under the high refractive index medium is consistent with the results of Mie theory.[18] The diffusion rate of each Au@SiO_2 yolk-shell nanoreactor could be calculated from the peak shifts versus time (see Experimental). As shown in Table 1, the diffusion coefficient of silica shells increases monotonically from 5.9×10^{-19} to 2.1×10^{-18} $m^2\ s^{-1}$ with an increase in [C_{18}TMS]/[TEOS]. This reveals that the introduction of C_{18}TMS as a porogen dictates the silica shell porosity of the Au@SiO_2 nanoreactor frameworks. The silica shells without C_{18}TMS exhibit a negligible diffusion coefficient after calcination. However, the same Au@SiO_2 particles before heat treatment have a diffusion rate of 4.7×10^{-19} $m^2\ s^{-1}$, comparable to the value ($\sim 4.76 \times 10^{-19}$ $m^2\ s^{-1}$) of the polymer shells in Au@PBzMA (poly(benzyl methacrylate)) particles.[5,19] This decent diffusion rate is attributed to sparsely polymerized sites and defects of the amorphous silica, which can be completely sealed by high temperature calcination.

Catalytic Reduction of *o*-Nitroaniline by Diffusion-Controlled Au@SiO_2 Yolk−Shell Nanoreactors. The catalytic reduction of aromatic nitrocompounds by $NaBH_4$ has been widely studied in the presence of coinage metals such as gold, silver, and copper.[15] This reaction is interpreted by an electron relay mechanism. The metal surface can transfer electrons from BH_4^- to the reactants, because metals have potentials lying between those of the donor (BH_4^-) and the acceptor (aromatic nitrocompounds). The reduction of *o*-nitroaniline (*o*-NA) to benzenediamine[20] by $NaBH_4$ was chosen as a model reaction for the diffusion-controlled Au@SiO_2 nanoreactor frameworks. This reaction did not occur without Au@SiO_2 catalysts during a period of more than two days. The same number of catalyst particles (1.1×10^{10}) was used for each reaction. A typical change of the UV−vis absorption during the reaction is shown in Figure 4a. The characteristic strong UV−vis peaks of *o*-NA appeared at 410 and 280 nm. As the reaction proceeded, the 410 nm peak completely disappeared, whereas the 280 nm peak was shifted to 290 nm within 20 min in the presence of Au@SiO_2 catalysts. This reaction could be analyzed by pseudofirst order kinetics, because excess $NaBH_4$ was used and thus the BH_4^- concentration was essentially constant throughout the reaction.

The turnover frequencies (TOFs), defined as moles (or numbers) of the product molecules generated per moles (or numbers) of catalyst surface atoms, were estimated for the Au@SiO_2 yolk−shell nanoreactors (Table 1). The Au@SiO_2 catalysts prepared without C_{18}TMS could not run the reaction due to complete coverage of the gold cores by the silica shells. With an increase of porosity in the silica shells, the gold surface is completely accessible by the solvent and reaction mixture, and the TOFs of the reactions mainly depend on the diffusion rate of the silica layers. The TOF increases rapidly from 5.1 to 35 with an increase of [C_{18}TMS]/[TEOS] from 0.06 to 0.12, which is a quantitative indication of the shell porosity. These results indicate that fast supply of the reactants on the catalyst surface gives high reaction rates within the same period.

The reaction progress was monitored by taking a small portion of the reaction mixture at a regular time interval of 3 min. The ratio of C_t and C_0, where C_t and C_0 are *o*-NA concentrations at times t and 0, was measured from the relative intensity ratio of the respective absorbance, A_t/A_0, at 410 nm. The linear relationship of $\ln(C_t/C_0)$ versus time

(18) Giersig, M.; Ung, T.; Liz-Marzan, L. M.; Mulvaney, P. *Adv. Mater.* **1997**, *9*, 570.
(19) Kreigbig, U.; Vollmer, M. *Optical Properties of Metal Clusters*; Springer: New York, 2004.
(20) Sau, T. K.; Pal, A.; Pal, T. *J. Phys. Chem. B* **2001**, *105*, 9266.

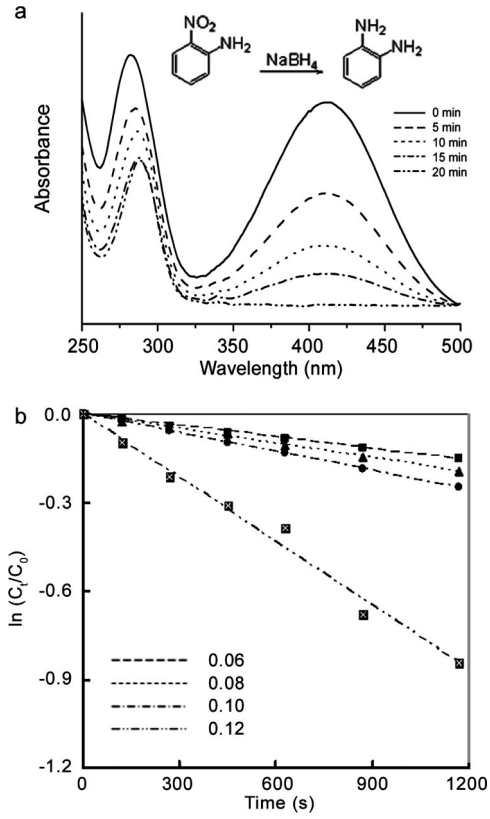

Figure 4. (a) Time-dependent UV−vis spectral changes of the reaction mixture catalyzed by diffusion-controlled Au@SiO$_2$ nanoreactors ([C_{18}TMS]/[TEOS] = 0.12). (b) Plots of ln(C_t/C_0) versus time and the rate constants (k_{obs}) for yolk−shell nanoreactor catalysts.

Table 2. Rate Constants (k_{obs} and k) for Au@SiO$_2$ Yolk−Shell Nanoreactor Frameworks[a]

[C_{18}TMS]/[TEOS]	k_{obs} (s^{-1})	k_{Au} (s^{-1})
0.06	1.3×10^{-4}	1.1×10^{-3}
0.08	1.6×10^{-4}	1.4×10^{-3}
0.10	2.1×10^{-4}	1.3×10^{-3}
0.12	7.2×10^{-4}	1.4×10^{-3}

[a] The same number of particles (1.1×10^{10}) was used for each reaction.

was observed for the yolk−shell catalysts, indicating that the reactions followed first-order kinetics. The observed rate constant (k_{obs}) for each catalyst was estimated directly from the slope of the straight line in Figure 4b. The Au@SiO$_2$ nanoreactor frameworks could be simplified as a combination of active gold nanoparticles and silica diffusion layers, and the rate constants on the gold surface (k_{Au}) were calculated from diffusion-coupled first-order reaction kinetics (see Experimental Section). The estimated k_{obs} and k_{Au} for the reactions are represented in Table 2. The k_{obs} increases 5.5 times from 1.3×10^{-4} to 7.2×10^{-4} s^{-1} with the increase of shell porosity. However, the k_{Au} values of the catalysts are nearly constant ($\sim 1.3 \times 10^{-3}$ s^{-1}), meaning that the etched gold cores in the Au@SiO$_2$ yolk−shell catalysts have regular particle sizes and surface morphology. It also matches with the fact that k_{Au} is essentially independent upon the diffusion rate of silica shells. Pal et al. reported the size selective reduction of *p*-nitrophenol by supported gold nanoparticles,[21] and concluded that the size and surface roughness are primary factors for the reaction rates. Smaller particles showed higher reactivity due to the large fraction of coordinatively unsaturated surface atoms. We have also observed similar size dependency of the Au@SiO$_2$ yolk−shell catalysts even though the core sizes are relatively large.[5] In this experiment, the catalysts were treated under the same experimental conditions to maintain the size of gold cores nearly identical (76−80 nm) and thus exhibited constant reduction rates on the gold surface.

Tuning of Surface Functionality of the Gold Cores in Au@SiO$_2$ Nanoreactors. Another strategy for improving catalytic efficiency is introducing specific functional groups on the metal surface. Bifunctional ligands containing thiol groups are likely to functionalize a gold surface through the formation of stable self-assembled monolayers (SAMs).[22] For the catalytic reduction of *o*-NA, an appropriate amount of 3-mercaptopropionic acid (3-MPA) was added to the diffusion-controlled Au@SiO$_2$ yolk−shell nanoreactors with a maximum porosity. The reaction mixture was stirred for 24 h at room temperature, and the excess thiol ligands were thoroughly washed with ethanol after the reaction. The TEM image in Figure 5a shows that the morphology of the Au@SiO$_2$ yolk−shell particles is unchanged after functionalization.

The resulting Au@SiO$_2$ catalysts carried out *o*-NA reduction with $NaBH_4$. Figure 5b represents the rate constant (k_{obs}) change by the functionalization of gold cores. The k_{obs} value of the standard Au@SiO$_2$ yolk-shell catalysts was 5.8×10^{-4} s^{-1}, depicted as a dotted line for comparison. The reaction rate increases dramatically at the low concentration range of 3-MPA up to 2.0 mmol, and reached a maximum rate of 1.4×10^{-3} s^{-1}, which is 2.4 times larger than that of the unfunctionalized core. The k_{obs} value then decreases slowly, and approaches the low limit of 1.5×10^{-4} s^{-1} at high concentrations of 3-MPA. Under the employed experimental conditions, the solution pH is nearly constant ($\sim$13) due to the excess amount of $NaBH_4$ in the reaction mixture. Therefore, most of the functional groups exposed on the surface are carboxylate anions,[23] which may form strong hydrogen bonding with the amine groups of *o*-NA.[23] This provides a relatively long reactant retention time and generates large concentration gradients around the active gold surface, yielding high k_{obs} values.

The reaction occurs at the exposed surface of the gold cores. At high concentrations of 3-MPA, the surface functional groups begin to form closed-packed domains and partially block the bare gold surface.[24] Consequently, the reaction rate approaches the maximum point and diminishes slowly as the surface functionality increases because of a combination of interaction with the reactants and blocking of the bare surface. The gold surface is completely blocked by excess thiols when 6.0 mmol of 3-MPA was used. It is assumed that 3-MPA molecules form ideally closed-packed

(21) Panigrahi, S.; Basu, S.; Praharaj, S.; Pande, S.; Jana, S.; Pal, A.; Ghosh, S. K.; Pal, T. *J. Phys. Chem. C* **2007**, *111*, 4596.
(22) Chechik, V.; Crooks, R. M.; Stirling, C. J. M. *Adv. Mater.* **2000**, *12*, 1161.
(23) Gershevitz, O.; Sukenik, C. N. *J. Am. Chem. Soc.* **2004**, *126*, 482.
(24) Cecchet, F.; Rudolf, P.; Rapino, S.; Margotti, M.; Paolucci, F.; Baggerman, J.; Brouwer, A. M.; Kay, E. R.; Wong, J. K. Y.; Leigh, D. A. *J. Phys. Chem. B* **2004**, *108*, 15192.

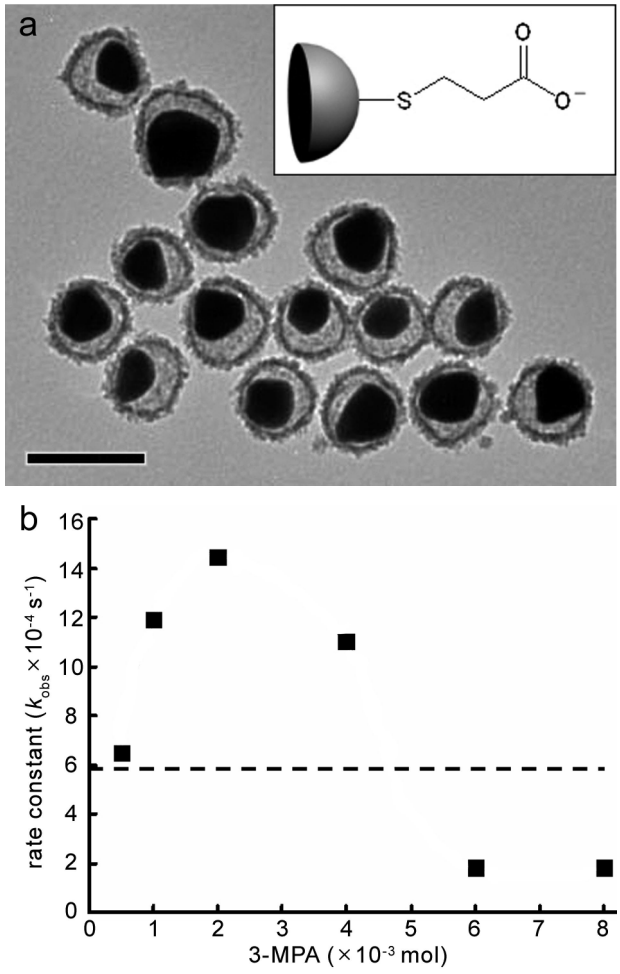

Figure 5. (a) TEM image of $Au@SiO_2$ yolk−shell nanoreactors after the addition of 3-MPA. The bar represents 200 nm. (b) Plot of the rate constants versus the amounts of 3-MPA used for functionalization. The dotted line represents the rate constant (5.8×10^{-4} s^{-1}) for diffusion-controlled $Au@SiO_2$ nanoreactors without 3-MPA.

SAMs at this point, where the number density of 3-MPA is simulated as 4.7×10^{14} molecules cm^{-2}, as reported in the literature.[25,26]

(25) Badia, A.; Cuccia, L.; Demers, L.; Morin, F.; Lennox, R. B. *J. Am. Chem. Soc.* **1997**, *119*, 2682.
(26) Tan, H.; Zhan, T.; Fan, W. Y. *J. Phys. Chem. B* **2006**, *110*, 21690.

It is remarkable that functionality on the metal surface significantly influences the reaction rates. Carboxylate groups on the gold surface could vary the reaction rate constants such that they were 2.4 times larger at maximum, and 4 times smaller at minimum relative to those of the unfunctionalized catalysts. In comparison with the original $Au@SiO_2$ yolk−shell nanoreactor framework without any chemical treatment ($k_{obs} = 1.1 \times 10^{-4}$ s^{-1}), this $Au@SiO_2$ catalyst with controlled diffusion and surface functionality exhibits a 13-fold enhanced rate constant.

Conclusion

Chemical tuning of $Au@SiO_2$ nanoreactor frameworks was found to be a very effective means of increasing the reaction rates of *o*-NA reduction. Introduction of C_{18}TMS to the reaction mixture altered the diffusion rates of silica shells 5-fold. The TOFs and rate constants were also significantly changed. The gold cores of $Au@SiO_2$ yolk−shell catalysts were selectively functionalized by the addition of 3-MPA, which generated carboxylate anions on the surface. The rate constant of *o*-NA reduction was enhanced 2.4 times compared to the unfunctionalized catalysts, and was 13 times larger than that of the original $Au@SiO_2$ catalysts prepared without C_{18}TMS. It is anticipated that these nanoreactor frameworks, in combination with chemical functionalization, have the potential to serve as a general platform for solution and gas phase reactions. Synthesis of the nanoreactor frameworks with various metals (Pd, Ni, Pt, etc.) is in progress in order to develop high-performance catalysts specific for chemically important reactions, such as hydrogenation, C−C coupling, and energy conversion.

Acknowledgment. This work was supported by Korea Science and Engineering Foundation (KOSEF) grants funded by the Korean government (MEST) (R01-2007-000-10570-0 and R11-2007-050-04002-0).

CM801149W